Materials Today Communications 35 (2023) 106323

Contents lists available at ScienceDirect

Materials Today Communications

journal homepage: www.elsevier.com/locate/mtcomm

Enhanced hydrophobicity of CeO_2 thin films: Role of the morphology, adsorbed species and crystallography

D. Mamedov [a], A.C. Åsland [b], S.P. Cooil [c], H.I. Røst [b], J. Bakkelund [b], A. Allaniyazov [d], J.W. Wells [b,c], S. Karazhanov [a,*]

[a] Department for Solar Energy Materials and Technologies, Institute for Energy Technology, 2027 Kjeller, Norway
[b] Center for Quantum Spintronics, Department of Physics, NTNU Norwegian University of Science and Technology, NO-7491 Trondheim, Norway
[c] Department of Physics/Centre for Materials Science and Nanotechnology, University of Oslo, N-0318 Oslo, Norway
[d] Department of Physics, Karakalpak State University, 230112 Nukus, Uzbekistan

ARTICLE INFO

Keywords:
Cerium dioxide
Sputter deposition
Superhydrophobicity
Surface texturization

ABSTRACT

In order to guarantee the long-term efficiency of hydrophobic materials in real-world situations, it is necessary that their surfaces are highly resistant to scratching, fouling and misting. Furthermore, for the specific applications, e.g. in photovoltaic systems, the water-repelling material must necessarily have a large bandage, such that it does not absorb light in the spectral range which is utilized by the underlying photovoltaic cell. One especially promising candidate for this and many other technologically important applications is cerium dioxide (CeO_2, ceria). In the current study, we propose the production framework for the manufacturing of CeO_2-based thin films with tunable wetting behavior. For obtaining the coatings with various hydrophobicity, ceria is deposited on the substrates with different roughness via reactive magnetron sputtering, with consequent treatment of the films in vapor of different hydrocarbons. By systematic study using the XRD, SEM, XPS and water contact angle (WCA) instruments, we found that surface texturization, different plains at the surface of the films as well as the adsorbed organic molecules all strongly influence on wettability of the CeO_2 thin films. In addition, comparison of WCAs for ceria and silicon oxide SiO_x is performed. The higher wettability for the former points out the essential role of the surface material despite presence of hydrocarbons. It is demonstrated that by purposeful controlling for all the parameters – surface texturization, the top material and its crystallography, and adsorbed organic molecules – one can reach superhydrophobic state of the surface.

1. Introduction

In the current glass market, there is a great need for inorganic materials that are mechanically strong with respect to mechanical wearing, which can withstand high temperature processing, and possess reduced wettability with large water contact angles. Such materials are especially important for applications in photovoltaic panels installed in rainy or high humidity areas, windows of buildings, automobiles, etc.

Rare-Earth metal oxides (REOs) possess hydrophobic properties [1]. Cerium is the most abundant lanthanide in the Earth's crust and it's dioxide (CeO_2, ceria), exhibits a large bandgap (around 3.0–3.6 eV [2–4]) and good mechanical stability [5], thus making this material promising for the above-mentioned applications. The original explanation of the ceria wetting behavior was based on its electronic structure [1]. According to that explanation, valence electron orbitals of the cerium atoms in CeO_2 are protected by the electron octet 2 $s^2 2p^6$ of crystalline oxygen which makes it difficult for water molecules to build chemical bonds with the surface. Later studies found, however, that as-prepared REOs show intrinsic hydrophilicity, and attributed high water contact angles (WCA) to adsorption of hydrocarbons which often are present in indoor air and pump systems [6–9]. Surface cleaning with high temperature annealing or with plasma treatment is able to switch the wetting behavior of REOs from hydrophobic to hydrophilic [10,11]. However, hydrophobic behavior of CeO_2 persists during and after UV-exposure due to lack of the surface self-cleaning from attached species [12], which makes transparent ceria suitable for outdoor applications. The hydrocarbon adsorption usually occurs at surface defects such as oxygen vacancies and adsorbed -OH groups, or by physical adsorption on the locally ideal surface [10]. However, it is not clear, if the adsorbed molecules dominate over intrinsic nature of CeO_2 in

* Corresponding author.
E-mail address: smagul.karazhanov@ife.no (S. Karazhanov).

https://doi.org/10.1016/j.mtcomm.2023.106323
Received 23 March 2023; Received in revised form 6 May 2023; Accepted 26 May 2023
Available online 29 May 2023

regulation of its wetting behavior [13], if the adsorption is reproducible and if it is permanent with respect to alteration of the original wetting behavior and enabling superhydrophobic or superhydrophilic states [14]. For a proper discrimination of the effect for the surface material and adsorbed species, it is required a constancy in the surface adsorption process represented by the adsorbate type and adsorbance conditions.

Enhancement of the wetting nature can be promoted by the advanced surface morphology which effect is described by Wenzel or Cassie-Baxter models [15]. Achievement of the well-defined parameters for the surface features then remains of great importance and is often accompanied with the technological challenges when applied for the different materials. Various approaches can be implemented for creation of desired surface patterns with controllable parameters, including laser ablation [16,17], selective etching or deposition of new material [18], spray-coating of particles [19], etc. However, most of the production methods applied directly to the hydrophobic or hydrophilic surface are high cost, time consuming, or can be implemented only to the specific materials. From this perspective, creation of the surface roughness on substrate with consequent covering with the studied layer can become a promising universal way towards controlled morphology, instead of manipulations with the top material [20]. Such approach allows production of different materials with comparable surface parameters for systematic study of their wetting behavior and other surface properties. For example, applying of micropillar structures to substrate allows hydrophobic yet sticky coatings after deposition of CeO_2 on them [21]. Moreover, the concept of manipulation with morphology of substrates, rather than hydrophobic material itself, could be expanded to porous 3D-structures enabling large opportunities for selective removal wastes from water [22].

In the current study, we implement an easy-to-scale method on the wet-etching Si-substrate texturization with following consequent deposition of CeO_2 by reactive magnetron sputtering and different hydrocarbons by thermal evaporation. The obtained surfaces demonstrate superhydrophobic behavior. We show that simultaneous effect of different factors such as surface morphology, adsorbed organic molecules, and crystallography of the CeO_2-film surface are needed for controlling the wetting behavior. Thus, the production method for CeO_2-based thin films proposed in the study can be easily adopted for getting the surfaces with large range of the observable WCAs.

2. Results and discussion

2.1. SEM and XRD measurements

The SEM micrograph of the texturized thin film surface is shown in Fig. 1. Applying the KOH-treatment to the monocrystalline Si substrates creates a pyramidal morphology of the surface. This effect is a result of anisotropic etching where different crystallographic planes are removed with different rates [23]. The surface of the pyramids is formed by Si (111) planes. Deposition of ceria thin films on top of the etched silicon does not change the morphology of the surface [Fig. 1(a)]. This occurs due to the relatively small thickness of the film compared with the typical size of the features on the substrate, allowing CeO_2 to inherit the surface roughness. Results on the EDX analysis, represented in Table S1 in Supplementary Information, confirm presence of Ce- and O-atoms on the surface. Applying of chemical polishing with solution of nitric, hydrofluoric and acetic acids (CP5-process) to the monocrystalline Si-wafer creates a non-periodic pattern on the surface as it is demonstrated in Fig. 1(b). Due to variations in the typical size and morphology for the surface features of Si-substrate, it is possible to demonstrate their importance for alteration of wetting properties for topmost CeO_2-layer. The deposited film of CeO_2 repeats the surface morphology of the

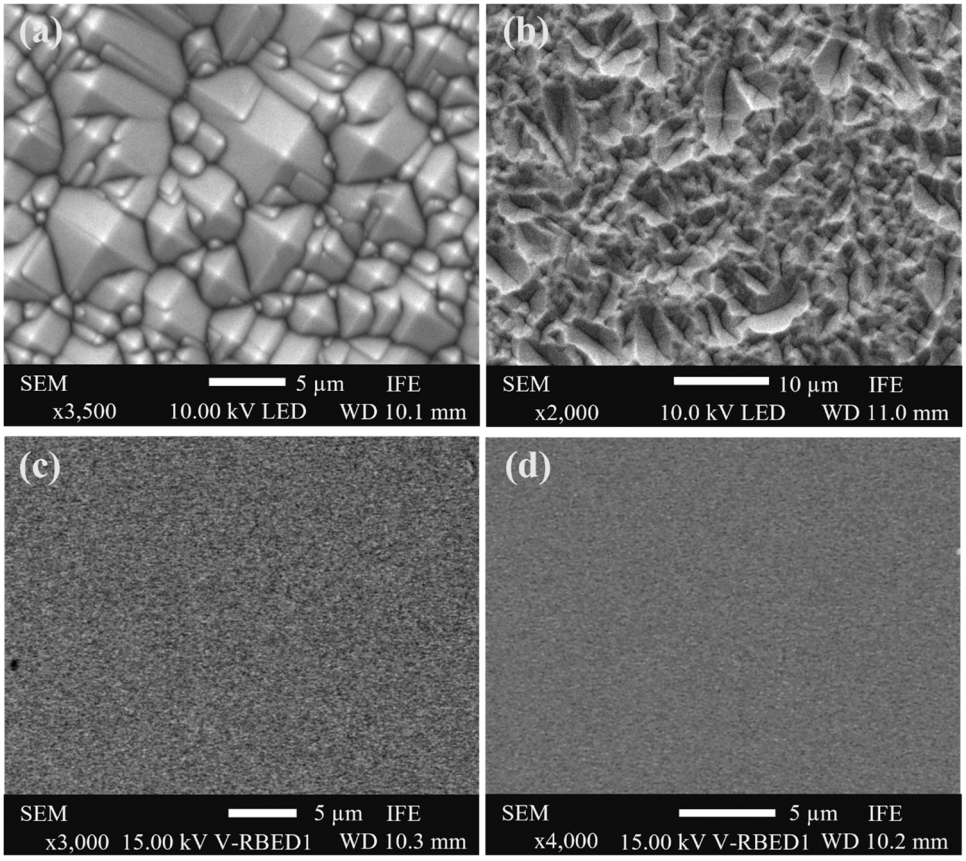

Fig. 1. SEM micrographs of CeO_2 thin film deposited on (a) Si-substrate treated with KOH-process, (b) CP5-process, (c) flat Si-substrate and (d) flat glass taken with low magnification.

substrate as it takes place for KOH-treatment. Utilization of Si and glass flat substrates for coating leads to the homogenous film of CeO_2, as it is shown in Fig. 1(c, d), respectively. High magnification micrographs for the flat coatings represented in Fig. S1 in Supplementary Information reveals the columnar structure of the thin films which remains featuring for the sputtered CeO_2 [24,25]. The typical size of the columns estimated from SEM pictures can be found in range 30–50 nm.

Results of the XRD measurements for the CeO_2 coatings deposited on flat Si and glass substrates are shown in Fig. 2. The patterns obtained for both cases indicate presence of the *fcc* fluorite structure of CeO_2. The peak at $2\theta \approx 33^\circ$ for the film deposited on Si-substrate appears as combination of signals from CeO_2 (200) and Si (200) planes. The reflection from the latter is forbidden for the ideal Si crystal, and when it occurs it may indicate lattice distortion of the substrate [26]. Analysis with Debye-Scherrer equation applied to peak (111) reveals the average crystalline size to be 15 nm. The lattice parameter is found according to the Bragg equation as a= 5.41 Å which corresponds well with the reported value of 5.411 Å (JCPDS No. 34–0394). Domination of the peak (200) for CeO_2 film on the glass substrate (red curve in Fig. 2) points out on the prioritised grain growth along [100] direction during deposition. The positions of the XRD peaks for CeO_2-film on glass is found shifted towards lower angles giving enhanced lattice parameter a= 5.43 Å, and crystalline size ~35 nm.

2.2. Wettability

2.2.1. Influence of organic material type on wettability

Dependences of the WCA for the CeO_2 deposited on the texturized and flat Si with deposited silicone oil (SilOil) and 1-octadecene are shown in Fig. 3(a) and (b), respectively. The initial values of WCA for the as-deposited ceria stay below 60° regardless substrate used, defining the surface as hydrophilic. Such wetting behavior corresponds well with numerous works [7–9,13,27–30] and confirms the idea of the intrinsic hydrophilicity of CeO_2. The obtained results demonstrate a significant increase of the hydrophobicity after deposition of the carbon containing molecules. For both types of the deposited organic materials, WCA exceeds 90° and transforms the ceria surface to the hydrophobic state. The saturation of the WCA values for the 1-octadecene occurs faster than that for the silicone oil, however the maximum achieved values remain lower for both the texturized and flat thin film.

Organic layer strongly influences on wettability of CeO_2. Thickness of the layer is not large enough and thus cannot be measured accurately with profilometer or SEM. For example, sub-nanometer thick 1-octadecene has been formed on graphite after 2 h deposition at room temperature [31]. Thickness of PDMS deposited by thermal evaporation at 234 °C for 30 min was found around 3 nm [32], which also limits that of silicone oil deposited at 100 °C within one nanometer. Such thin layers

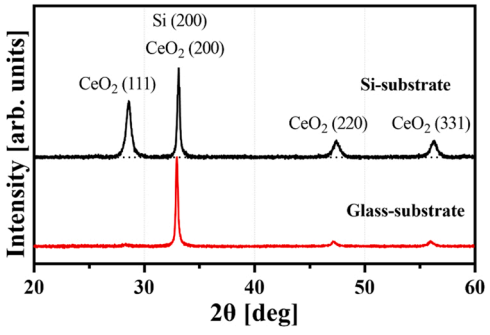

Fig. 2. XRD patterns of CeO_2 thin film deposited on flat Si (black curve) and glass (red curve) substrates in the scan range 20–60°, identified peaks for CeO_2 are labeled corresponding to JCPDS No. 34–0394. Peak (200) for CeO_2 deposited on Si experiences overlapping with forbidden peak (200) for Si-substrate.

of organic molecules strongly influence on wettability of CeO_2. Surface tension of the coating can be represented as product of that for the organic material and CeO_2. According to the Young equation, enhanced hydrophobicity indicates a lower surface energy for the silicone oil which stimulates reduction of the total interface area between water and ceria. Surface tension of polydimethylsiloxane (PDMS), the main component for the silicone oil used in the current study, is found to be in the range 19–21 mN/m [33] whereas that for 1-octadecene 29.2 mN/m [34]. According to Owens-Wendt-Rabel-Kaelble (OWRK) model [35], the decrease in dispersive (upper index D in Eq. (1)) and polar (upper index P in Eq. (1)) components of surface tension γ_S for thin film is resulted in higher contact angle as following:

$$\gamma_L(1+\cos\theta) = 2\left[\left(\gamma_S^D\gamma_L^D\right)^{1/2} + \left(\gamma_S^P\gamma_L^P\right)^{1/2}\right] \quad (1)$$

where γ_L is the surface free energy for liquid (water). It indicates that deposition of organic molecules with lower surface tension enhances WCA of CeO_2.

Texturization with KOH-treatment enhances the initial hydrophobicity of the CeO_2 surface no matter what contaminator was used. It should be noted that in this case silicone oil deposition on the surface allows superhydrophobicity of the CeO_2 with contact angles around 162°. The lower roughness achieved by the CP5-treatment polishing (orange curves in Fig. 3) possesses no significant change in the values of WCA comparing with the flat substrate. The results obtained suggest sensitivity of the wetting behavior of CeO_2 films on their surface morphology.

Applying the adsorption process of the organic molecules allows to achieve three different goals. The first one is related to the time of saturation for wetting properties. In various works [6–8,13,29], the period of establishment for the hydrophobic state of CeO_2 and other REOs is found in the large range from days to months. Applying the deposition process in a saturated environment allows the completion time to be reduced from days to hours. This time can be controlled by the temperature of the process which governs the vapor pressure of the organic material. The second advantage is in the reproducibility of the results over different experiments since the deposition environment remains constant. The last advantage of using a controlled environment is the ability to modify the final wetting properties of the material using various substances, including those which cannot be found in atmosphere or vacuum chambers.

From Fig. 3, a significant change can be detected in the WCAs values for the flat glass and Si-substrates, especially after treatment in the silicon oil vapor. This change in the hydrophobicity is essentially determined by the surface crystallography of the thin film, as it is observed from XRD patterns in Fig. 2. To confirm the influence of the different crystallographic surfaces of CeO_2 on hydrophobic properties and avoid possible effect of the substrate, we produced depositions of CeO_2-films on glass substrate at the elevated temperature and different pressures (see Experimental details). Fig. 4 represents the XRD patterns of obtained thin films of CeO_2 and appearance of droplets on the material surfaces after deposition of SilOil for 17 h at 100 °C.

Analysis of the XRD patterns represented in Fig. 4 indicates existence the preferable direction of the film growth at both deposition pressures. For the thin films of CeO_2 prepared at the lower pressure (0.5 Pa, upper plot in Fig. 2(a)), the pattern possesses domination of the (200) peak. Therefore, the flat film surface is mostly formed for the (100) crystallographic plane. This structure is similar to the films prepared at same pressure and room temperature (red curve in Fig. 2). Increasing of the chamber pressure to 1.0 Pa stimulates formation of the (111) surface as shown in the lower plot in Fig. 4(a). Comparison of the wetting properties for CeO_2 after deposition of SilOil, reveals lower values of WCA for the films with surface (200) than the films with surface (111) with contact angles (114.5 ± 3.4)° (Fig. 4(b)) and (132 ± 5.8)° (Fig. 4(c)), respectively. The relationship $\theta_{(111)} > \theta_{(200)}$ is due to different surface free energy for the selected plains [Eq. (1)] and is consistent with the

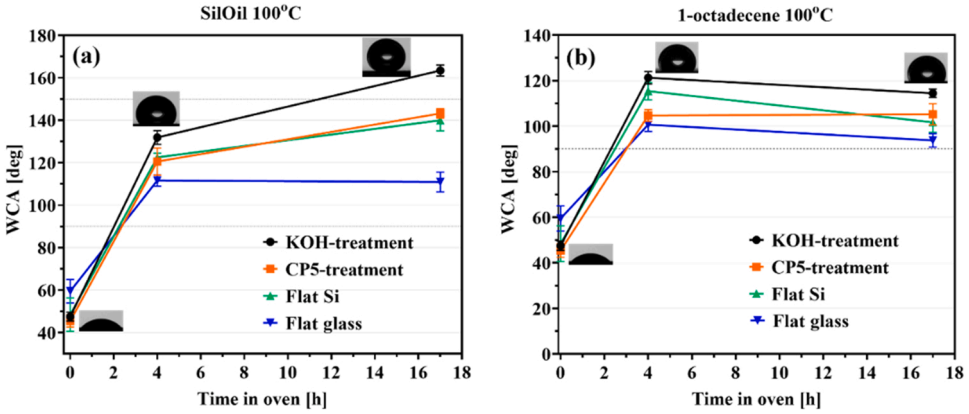

Fig. 3. Dependence of WCA on time of organic molecules deposition for (a) silicone oil and (b) 1-octadecene. Dashed lines indicate thresholds for the hydrophobic (90°) and superhydrophobic (150°) conditions. Appearance of droplets is shown for CeO_2 films deposited on the KOH-treated substrate (images for all the points can be found in Fig. S2 and S3 in Supplementary Information).

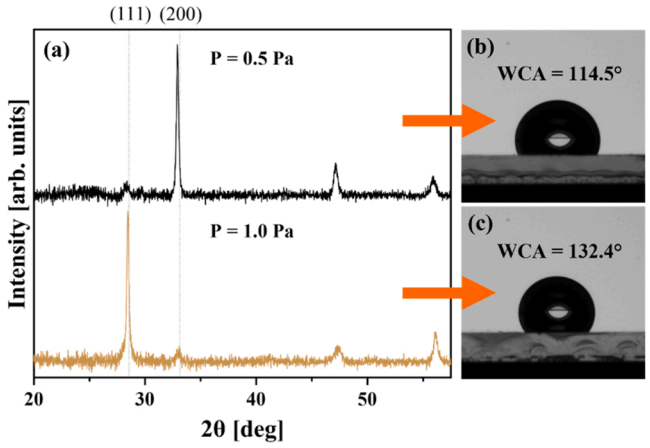

Fig. 4. (a) XRD patterns of the CeO_2 thin films deposited on the glass substrate at the different chamber pressures. Dashed vertical lines represent peak positions for the the crystallographic planes labeled above, according to the reference pattern (JCPDS No. 34–0394). (b, c) Appearance of the water droplets on the CeO_2 films deposited at chamber pressure of 0.5 Pa and 1.0 Pa, respectively.

results of Ref. [28] about hydrophobicity of different planes of CeO_2 with airborne organics. Dependence of WCA on the surface crystallography of CeO_2 films was also observed after spontaneous adsorption of hydrocarbons [36]. Theoretical considerations for bare CeO_2 low-index surfaces attribute the variation in WCA to the difference in adsorption energy of water layers near the surface [37]. The influence of the crystallography apparently persists despite presence of the adsorbed molecules on the surface. Due to relatively high partial pressure of the silicone oil vapor during the heat treatment step and sufficient time for their deposition on surface of CeO_2 (17 h), in both cases we assume the saturation of the thin film surface by hydrocarbons. It should also be mentioned that different deposition parameters of the sputtering unit can also influence on the nanoscale surface roughness (RMS) of the films [38]. Indeed, a correlation between RMS of sputtered films of CeO_2 and their WCAs was suggested previously in literature [39,40]. However, this effect can be additionally attributed to thickness of ceria coatings, which makes the influence of the sputtering-induced roughness less prominent [5]. Moreover, the other studies about CeO_2 films of fixed thickness and controlled RMS revealed no clear correlation between nanoscale roughness and WCAs [41,42]. Furthermore, thin films of CeO_2 deposited on flat Si and glass at identical parameters possess different preferential orientation for grains with extra contribution of (111) plains for the former [Fig. 2]. At the same time, ceria-films deposited on Si-substrate still demonstrate higher WCAs [Fig. 3], which confirms the general trend on the enhancement of hydrophobicity with (111)-surface. Therefore, the observable change in the values of WCA for samples with different crystallography can be attributed directly to the characteristics of CeO_2 surface.

2.2.2. *Influence of surface materials*

To summarize the influence of the different factors on the wetting properties of the surfaces, WCA for samples with and without deposited CeO_2 have been compared, with and without silicone oil present. The comparative diagram of the wetting properties for different types of surfaces is shown in Fig. 5. For each type of substrate topology, we considered 4 different situations: deposited ceria and SilOil (black bars), substrate without ceria but with SilOil (red), ceria without SilOil (blue) and bare substrate without SilOil (grey). Schematic representation of the studied cases is shown in Fig. S4 in Supplementary Information. All depositions of the silicone oil have been carried out for 17 h. Analysis shows that the presence of the ceria thin film increases WCA regardless of the presence of the attached organic molecules on the surface (black and red, blue, and grey columns within one group for samples with and without SilOil, respectively). The surface of the substrate without ceria

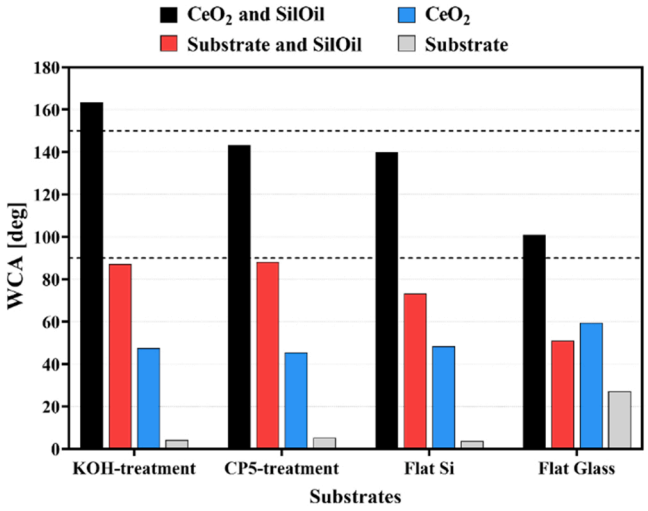

Fig. 5. Comparative diagram of the WCA for different substrates with and without adsorbed organic molecules. KOH-treatment and CP5-treatment groups represents surfaces texturized with the corresponding methods. Dashed lines indicate thresholds for the hydrophobic (90°) and superhydrophobic (150 °) conditions.

(red and grey bars in Fig. 5) consists of the non-stoichiometric SiO_x, naturally formed by oxidation of silicon in the atmospheric air. Silicon oxide possesses hydrophilic behavior with contact angle less than 10°, corresponding well with the studies on the wetting properties of silica [6]. Applying the SilOil significantly increases hydrophobicity for any type of surface, however, the presence of the organic molecules with low surface energy does not make different materials equally water repelling. This fact points out the importance of the surface material in achieving the superhydrophobic condition.

2.3. XPS measurements

XPS spectra for the CeO_2 films are presented in Fig. 6. From the widescan [Fig. 6(a)], Ce and O peaks are observed, together with C and some Si from the substrate. Before the sample was heated in vacuum, the relative intensities of Ce4p:O1s:C1s were found to be 1:2:4, and after heating the ratios were 1:2:2. Hence, the intensity of the O 1 s and Ce peaks increases and the C 1 s peak decreases upon heating, indicating that some of the carbon contamination on the surface is released and more of the CeO_2 is seen. The spectra shift 1–3 eV towards lower binding energies after heating. When the thin film is heated in vacuum, oxygen may be emitted from the surface. This in turn may change the potential at the surface, possibly causing the observed shift in binding energy [43]. The binding energies given in previous work [44–47] are closer to those of the sample after it has been heated in vacuum, and the following discussion will hence be based on those values.

Fig. 6(b)-(d) show spectra of the O 1 s, C 1 s and Ce 4p peaks. The O 1 s spectra in Fig. 6(b) can be decomposed into three peaks with binding energy 530.2 eV (531.5 eV), 531.6 eV (533.5 eV) and 532.5 eV (534.6 eV) after (before) heating. The largest component at E_B= 530.2 eV is oxygen from the CeO_2 lattice, and this is the component increasing upon heating. The component at 531.6 eV has previously been assigned to hydroxyls or carbonates [44–46], and the peak at 532.5 eV may be from O bound to the Si-substrate or molecular water [45–47]. Since the Si 2p peak can be seen [Fig. 6(a)] even with a relatively thick film of CeO_2, the film is probably not uniform. It is likely that the substrate has reacted with oxygen to form SiO_2 during the preparation of the sample, and that some of this SiO_2 gives rise to the peak at 532.5 eV. The peak decreases upon heating, as is expected for both SiO_2 and adsorbed water. Heating may make the film more uniform, such that less of the SiO_2 is seen, or make water evaporate from the surface.

For the C 1 s peak in Fig. 6(c), the major component at binding energy 285.3 eV (287.2 eV) stems from a variety of hydrocarbons on the surface, as is expected for most samples exposed to air [48]. The peak at 287.0 eV (289.2 eV) is likely from carbon bound to oxygen in alcohols, ethers, ketones or aldehydes [45,48]. Ce 4 s is expected to be at a binding energy of 289 eV [47]. The peak at 289.7 eV (291.0 eV) in the C 1 s spectrum is therefore thought to be Ce 4 s, but it could also be carbonates [45].

The shape of the Ce 4p peak, seen in Fig. 6(d) resembles that found in literature [47]. Due to final state effects [47,49], the Ce 4p 3/2 peak is split into three peaks, P1 (turquoise), P2 (purple) and P3 (green), each

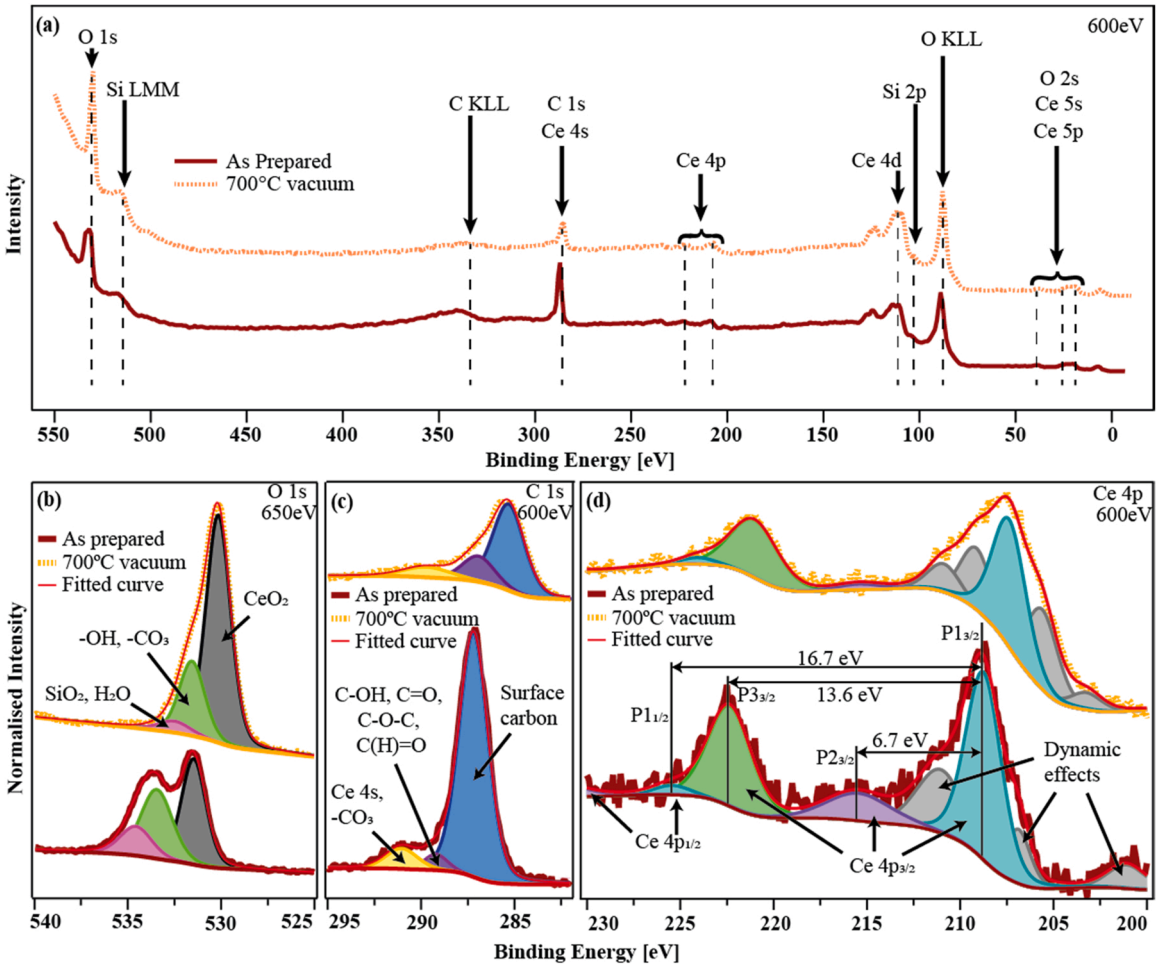

Fig. 6. XPS results from as prepared and annealed samples: (a) Widescan measured with photon energy 600 eV. (b)-(d) Narrow scans of O 1 s (b), C 1 s (c) and Ce 4p (d) core levels. The dark red line is the sample as it was loaded, and the orange dotted line after it had been heated to 700 °C in vacuum. The O 1 s (b) and C 1 s (c) spectra have been decomposed into peaks corresponding to different groups of molecules containing oxygen or carbon.

for a different final state. P2 and P3 are shifted from the P1 peak by 6.7 eV and 13.6 eV respectively, which is close to the shifts found in ref. [47]. The spin-orbit splitting of the Ce 4p is found to be 16.7 eV, which agrees with the expected value. The 4p ½ peak is shown for the P1 final state. If a surface layer of carbon is removed when heating (upper curve in Fig. 4(d)), the cerium intensity is expected to increase. However, from the narrow scan in Fig. 6(d), the intensity of the Ce 4p peak seems to not increase upon heating, and neither does the Ce 4 s peak in Fig. 6(c). This is probably because of uncertainty in the intensities for these scans. Due to low intensities, a higher pass energy (100 eV, instead of 40 eV) was used when acquiring spectra Ce 4p and C 1 s after heating. In Fig. 6(c) and (d), a scaling factor was utilized to obtain equivalent intensities before and after heating, but the uncertainty when comparing the intensity for these curves are greater than for the O 1 s spectra. When looking at the Ce 4p peaks before and after heating from the widescan in Fig. 6(a), the intensity of Ce 4p seems to have increased by a factor of 1.2 after heating.

3. Conclusions

In the current research effort, the different factors influencing the wettability of CeO_2 deposited by magnetron sputtering were studied. The chemical composition of the coatings was found as CeO_2 by means of XRD and XPS measurements and the texturization of the films was confirmed with SEM. Hydrophobicity of thin films of CeO_2 deposited by magnetron sputtering has systematically been studied. We have observed drastic enhancement of water contact angle of the films by surface texturization as compared to flat surface. Hydrophobicity of the films has further been enhanced by depositing silicone oil and 1-octadecene. Despite adsorbed molecules, presence of CeO_2 top layer significantly influences on hydrophobicity of the surface, in comparison with bare SiO_x. Moreover, different planes on surface of CeO_2-film also play a role towards control of WCA. In conclusion, surface texturization, surface material, and adsorbed organic molecules are the parameters that can be used for controlling water contact angle in a wide range and enabling the superhydrophobic state. They must be considered in a bundle to perform a fair comparison of different surfaces regarding the interaction with water.

4. Methods

4.1. Fabrication of superhydrophobic coating

The principal way to achieve the superhydrophobic state with WCA above 150° is through the creation of surface roughness by surface texturization [50]. It should be mentioned that besides helping to achieve the superhydrophobic condition, the advanced surface morphology reduces reflection from the material and therefore makes it advantageous for use in photovoltaic (PV) applications. For the bulk material, surface texturization can be performed within two different paradigms or one of their combinations [14]. The first one, "Top-Bottom", implies selective removal of material from the surface by etching or laser ablation [17]. The second approach, called "bottom-up", consists of deposition of new material on the surface, creating a new geometric pattern on top of it. As an example of the latter, for thin films deposited by sputter deposition, the surface roughness can be related to the substrate texturization if the typical size of the texture element is much more or comparable with the film thickness. In this case the deposited thin film inherits the texturization of the substrate which helps to modify wetting properties of the material.

The procedure for producing CeO_2-based superhydrophobic films utilized in this work consists of 3 consequent steps [Fig. 7]: 1) texturization of the substrate by chemical etching; 2) sputter deposition of a CeO_2 thin film; 3) controlled adsorption of organic molecules by placing the CeO_2 in a saturated environment of organic materials.

The substates used to obtain the superhydrophobic condition for

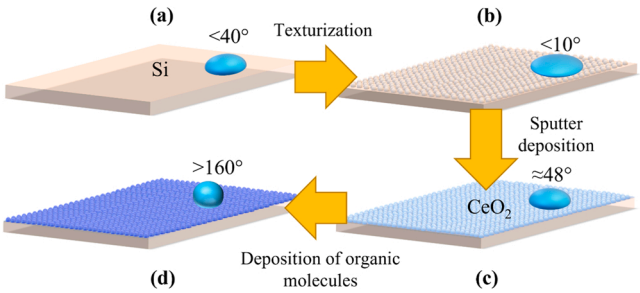

Fig. 7. Production procedure for CeO_2-based superhydrophobic coatings: (a) initial flat surface of the monocrystalline Si; (b) texturized surface of Si; (c) coating of CeO_2 deposited on texturized Si-substrate; (d) thin film of CeO_2 with adsorbed organic molecules. In all panels, the droplet shapes are shown schematically.

CeO_2 were monocrystalline (100) *n*-type silicon wafers with initial thickness d= 100 μm. In order to get even texturization of ceria thin films, the Si wafers were chemically etched using a KOH wet process [51]. The KOH concentration was maintained at a level of 2 wt% during etching., and was carried out at 80 °C for 20 min. To terminate the etch and remove any etchant remaining on the Si surface, the wafers were immersed in a 5% HCl solution for 120 s and subsequently rinsed with deionized water and dried using N_2 gas. The mass loss from the wafers was found to be roughly 6% of the initial value. Before deposition of ceria, the Si substrates were cleaned by ultrasonication in isopropanol for 10 min, rinsed with deionized water and dried in N_2 gas at room temperature. For the comparison, another process of chemical polishing of Si with mix of nitric, acetic and hydrofluoric acids, reffered as CP5-polishing, was used to obtain a substrate surface with a lower roughness [52]. In brief, a monocrystalline Si-wafer was immersed in the bath of acids (HNO_3:CH_3COOH:HF, 10:5:2 (vol.)) at room temperature for 60 s and then rinsed with water and dried in N_2. For the reference samples, we utilized non-treated flat Si wafers and flat slides of soda-lime glass (Menzel Gläser) as substrates.

The cerium dioxide thin films were deposited by DC reactive magnetron sputtering (Leybold A550V7 industrial type unit). The base pressure in the process chamber was maintained at $3*10^{-6}$ mbar. A cerium metal target of purity 99.5% was used in an argon-oxygen gas mixture with O/Ar inlet flow proportion at 31% and total pressure of 0.5 Pa. The substrate and the target were both kept at room temperature during the deposition process. The power density during the deposition process was 1.06 W/cm^2. The deposited thin films had a thickness of 200 nm for the flat substrate and was determined using a profilometer.

For confirmation of the role of crystallographic condition of CeO_2-film on the wetting behavior and exclusion the possible effect of the substrate material, we additionally performed sputter depositions of CeO_2 on flat glass substrate with different crystallographic orientation of the film surface. Such control of film structure can be achieved by change of the partial pressure of oxygen during the deposition process [38]. In the current study, the total pressure in the chamber was varied from 0.5 Pa to 1.0 Pa with keeping the same flow rates O/Ar= 31%. To avoid formation of high arcs during the reactive sputtering, the coating process was performed at the elevated temperatures of 200 °C for the substrate and 150 °C for the target. The thickness of the obtained films was determined at ~200 nm by the profilometer measurements. After the deposition of CeO_2, thin films were treated in the vapors of silicone oil for 17 h at 100 °C in air.

After CeO_2 deposition, the obtained thin films were covered with different organic materials by thermal evaporation performed in air. For this, samples were put in a polypropylene box with a liquid source of organic molecules before the closed and sealed box was placed in an oven at a temperature of 100 ℃ for durations up to 17 h. The organic materials used for the deposition were silicone oil (technical grade, type P20.275.50, Huber SilOil) and hydrocarbon 1-octadecene (technical

grade 90%, Sigma-Aldrich). Silicone oil, with polydimethylsiloxane (PDMS) as main component, is widely used in pump systems and can become a primary contamination agent of CeO_2 during storage of thin films in low-vacuum conditions. At the same time, 1-octadecene represents typical chain hydrocarbon which can be used for demonstration of surface modification effect of CeO_2 by airborne organic molecules [31].

4.2. Characterizations

XRD, SEM and WCA. The phase content of the obtained thin films was characterized by means W of XRD (Bruker D2 Phaser, Cu-Kα radiation). The scanning was conducted with Bragg-Brentano focusing, with 2θ in the range 20–60° to estimate the contribution of the main planes to the surface crystallography. To assess surface morphology after the film deposition, SEM study was performed (JEOL model JSM-7900 F). The wettability characterization was carried out with the sessile droplet method. Droplets of Milli-Q water were placed on the thin film surface with a manually controlled mechanical syringe with varying droplet volume in the range 8–12 μL. The water droplets on the surface were photographed using a high-speed camera. Image analysis and calculations of the contact angles were performed using the Attension Theta software. The final value of the contact angle for each sample was averaged over five independent measurements.

XPS. To confirm the elemental composition, X-ray photoelectron spectroscopy (XPS) was performed on a CeO_2 sample at the AU-MATLINE beamline of the ASTRID2 synchrotron, Aarhus University, Denmark. To reduce the probability of charging effects due to the insulating nature of CeO_2, a thinner film of 50 nm thickness was deposited on a flat Si substrate, without any consequent covering with organic materials. Measurements were performed in ultrahigh vacuum (pressure in the order of 10^{-10} mbar) and with photoexcitation energies 600 eV and 650 eV. The sample was measured as prepared, and after having been heated to 700 °C in vacuum.

CRediT authorship contribution statement

Conception and design of study: S. Zh. Karazhanov and J. W. Wells, acquisition of data: D. Mamedov, A. C. Åsland, S. Cooil, H. I. Røst, J. Bakkelund, A. Allaniyazov, analysis and/or interpretation of data: D. Mamedov, A. C. Åsland, S. Cooil, Drafting the manuscript: D. Mamedov, A. C. Åsland, J. W. Wells, and S. Zh. Karazhanov, revising the manuscript critically for important intellectual content: D. Mamedov, S. Zh. Karazhanov and J, W. Wells.Approval of the version of the manuscript to be published (the names of all authors must be listed), D. Mamedov, A. C. Åsland, S. Cooil, H. I. Røst, J. Bakkelund, A. Allaniyazov, J. W. Wells and S. Zh.Karazhanov.

Declaration of Competing Interest

The authors declare that they have no known competing financial interests or personal relationships that could have appeared to influence the work reported in this paper.

Data availability

No data was used for the research described in the article.

Acknowledgments

Authors acknowledge Rune Søndenå and Bent Andreas Thomassen from the Department of Solar Energy Materials and Technologies (SOLTEK) of the Institute for Energy Technology (IFE), for help with etching process and Elbruz Murat Baba (SOLTEK, IFE) for the productive discussions. This work was supported by the Norwegian Research Council through the projects 309827 and 262633 Centers of Excellence funding scheme. The authors acknowledge Dr. Zheshen Li and the staff of the ASTRID2 synchrotron in Aarhus, Denmark for practical assistance and discussions.

Appendix A. Supporting information

Supplementary data associated with this article can be found in the online version at doi:10.1016/j.mtcomm.2023.106323.

References

[1] G. Azimi, R. Dhiman, H.M. Kwon, A.T. Paxson, K.K. Varanasi, Hydrophobicity of rare-earth oxide ceramics, Nat. Mater. 12 (2013) 315–320, https://doi.org/10.1038/nmat3545.
[2] S. Guo, H. Arwin, S.N. Jacobsen, K. Järrendahl, U. Helmersson, A spectroscopic ellipsometry study of cerium dioxide thin films grown on sapphire by rf magnetron sputtering, J. Appl. Phys. 77 (1995) 5369–5376, https://doi.org/10.1063/1.359225.
[3] S. Colis, A. Bouaine, R. Moubah, G. Schmerber, C. Ulhaq-Bouillet, A. Dinia, L. Dahéron, J. Petersen, C. Becker, Extrinsic ferromagnetism in epitaxial Co-doped CeO2 pulsed laser deposited films, J. Appl. Phys. 108 (2010), https://doi.org/10.1063/1.3481026.
[4] R.M. Bueno, J.M. Martinez-Duart, M. Hernández-Vélez, L. Vázquez, Optical and structural characterization of r.f. sputtered CeO2 thin films, J. Mater. Sci. 32 (1997) 1861–1865, https://doi.org/10.1023/A:1018509007844.
[5] D. Zhu, X. Tan, L. Ji, Z. Shi, X. Zhang, Preparation of transparent and hydrophobic cerium oxide films with stable mechanical properties by magnetron sputtering, Vacuum 184 (2021), 109888, https://doi.org/10.1016/j.vacuum.2020.109888.
[6] D.J. Preston, N. Miljkovic, J. Sack, R. Enright, J. Queeney, E.N. Wang, Effect of hydrocarbon adsorption on the wettability of rare earth oxide ceramics, Appl. Phys. Lett. 105 (2014) 1–8, https://doi.org/10.1063/1.4886410.
[7] S. Prakash, S. Ghosh, A. Patra, M. Annamalai, M.R. Motapothula, S. Sarkar, S.J. R. Tan, J. Zhunan, K.P. Loh, T. Venkatesan, Intrinsic hydrophilic nature of epitaxial thin-film of rare-earth oxide grown by pulsed laser deposition, Nanoscale 10 (2018) 3356–3361, https://doi.org/10.1039/C7NR06642B.
[8] S.P. Fu, J. Rossero, C. Chen, D. Li, C.G. Takoudis, J.T. Abiade, On the wetting behavior of ceria thin films grown by pulsed laser deposition, Appl. Phys. Lett. 110 (2017) 1–6, https://doi.org/10.1063/1.4973997.
[9] Z. Shi, Z. Zhou, P. Shum, L.K.-Y. Li, Thermal stability, wettability and corrosion resistance of sputtered ceria films on 316 stainless steel, Appl. Surf. Sci. 477 (2019) 166–171, https://doi.org/10.1016/j.apsusc.2017.11.041.
[10] P. Xu, G. Meng, L. Pershin, J. Mostaghimi, T.W. Coyle, Control of the hydrophobicity of rare earth oxide coatings deposited by solution precursor plasma spray by hydrocarbon adsorption, J. Mater. Sci. Technol. 62 (2021) 107–118, https://doi.org/10.1016/j.jmst.2020.04.044.
[11] Y. Wang, Q. Zhou, L. Kang, L. Yang, H. Wu, Z. Zhou, C. Xiao, J. Guo, F. Yang, S. Zhang, G. Li, Y. Jin, Oxide-water interaction and wetting property of ceria surfaces tuned by high-temperature thermal aging, Appl. Surf. Sci. 554 (2021), 149658, https://doi.org/10.1016/j.apsusc.2021.149658.
[12] X.-P. Li, Y.-L. Sun, C.-W. Luo, Z.-S. Chao, UV-resistant hydrophobic CeO_2 nanomaterial with photocatalytic depollution performance, Ceram. Int. 44 (2018) 13439–13443, https://doi.org/10.1016/j.ceramint.2018.04.132.
[13] R. Lundy, C. Byrne, J. Bogan, K. Nolan, M.N. Collins, E. Dalton, R. Enright, Exploring the role of adsorption and surface state on the hydrophobicity of rare earth oxides, ACS Appl. Mater. Interfaces 9 (2017) 13751–13760, https://doi.org/10.1021/acsami.7b01515.
[14] J. Jeevahan, M. Chandrasekaran, G. Britto Joseph, R.B. Durairaj, G. Mageshwaran, Superhydrophobic surfaces: a review on fundamentals applications and challenges, J. Coat. Technol. Res. 15 (2018) 231–250, https://doi.org/10.1007/s11998-017-0011-x.
[15] D. Murakami, H. Jinnai, A. Takahara, Wetting transition from the cassie–baxter state to the wenzel state on textured polymer surfaces, Langmuir 30 (2014) 2061–2067, https://doi.org/10.1021/la4049067.
[16] A. Volpe, C. Gaudiuso, L. Di Venere, F. Licciulli, F. Giordano, A. Ancona, Direct femtosecond laser fabrication of superhydrophobic aluminum alloy surfaces with anti-icing properties, Coatings 10 (2020), https://doi.org/10.3390/COATINGS10060587.
[17] S.F. Toosi, S. Moradi, S.G. Hatzikiriakos, Fabrication of micro/nano patterns on polymeric substrates using laser ablation methods to control wettability behaviour: a critical review, Rev. Adhes. Adhes. 5 (2017) 55–78, https://doi.org/10.7569/RAA.2017.097302.
[18] P. Dimitrakellis, E. Gogolides, Hydrophobic and superhydrophobic surfaces fabricated using atmospheric pressure cold plasma technology: a review, Adv. Colloid Interface Sci. 254 (2018) 1–21, https://doi.org/10.1016/j.cis.2018.03.009.
[19] O.S.A. Rahman, B. Mukherjee, S. Priyadershini, M.R. Gunjan, R. Raj, S.T. Aruna, A. K. Keshri, Investigating the wetting phenomena and fabrication of sticky, para-hydrophobic cerium oxide coating, J. Eur. Ceram. Soc. 40 (2020) 5749–5757, https://doi.org/10.1016/j.jeurceramsoc.2020.06.028.
[20] K. Teshima, H. Sugimura, Y. Inoue, O. Takai, A. Takano, Transparent ultra water-repellent poly(ethylene terephthalate) substrates fabricated by oxygen plasma treatment and subsequent hydrophobic coating, Appl. Surf. Sci. 244 (2005) 619–622, https://doi.org/10.1016/j.apsusc.2004.10.143.

[21] Z. Shi, Z. Zhang, W. Huang, H. Zeng, V. Mandić, X. Hu, L. Zhao, X. Zhang, Spontaneous adsorption-induced Salvinia-like micropillars with high adhesion, Langmuir 37 (2021) 6728–6735, https://doi.org/10.1021/acs.langmuir.1c00702.
[22] Z. Shi, H. Zeng, Y. Yuan, N. Shi, L. Wen, H. Rong, D. Zhu, L. Hu, L. Ji, L. Zhao, X. Zhang, Constructing superhydrophobicity by self-assembly of SiO_2@ Polydopamine Core-Shell Nanospheres with Robust Oil-Water Separation Efficiency and Anti-Corrosion Performance, Adv. Funct. Mater. 2213042 (2023) 1–11, https://doi.org/10.1002/adfm.202213042.
[23] H. Seidel, L. Csepregi, A. Heuberger, H. Baumgärtel, Anisotropic etching of crystalline silicon in alkaline solutions: I. Orientation Dependence and Behavior of Passivation Layers, J. Electrochem. Soc. 137 (1990) 3612–3626, https://doi.org/10.1149/1.2086277.
[24] M.S. Kabir, P. Munroe, V. Gonçales, Z. Zhou, Z. Xie, Structure and properties of hydrophobic CeO2−x coatings synthesized by reactive magnetron sputtering for biomedical applications, Surf. Coat. Technol. 349 (2018) 667–676, https://doi.org/10.1016/j.surfcoat.2018.06.031.
[25] S. Phokha, S. Limwichean, M. Horprathum, V. Patthanasettakul, C. Chananonnawathorn, P. Eiamchai, N. Chanlek, S. Maensiri, Effect of annealing temperature on the structural and magnetic properties of CeO2 thin films, Thin Solid Films 704 (2020), 138001, https://doi.org/10.1016/j.tsf.2020.138001.
[26] L. Zhao, M. Steinhart, M. Yosef, S.K. Lee, T. Geppert, E. Pippel, R. Scholz, U. Gösele, S. Schlecht, Lithium niobate microtubes within ordered macroporous silicon by templated thermolysis of a single source precursor, Chem. Mater. 17 (2005) 3–5, https://doi.org/10.1021/cm0484302.
[27] J. Oh, D. Orejon, W. Park, H. Cha, S. Sett, Y. Yokoyama, V. Thoreton, Y. Takata, N. Miljkovic, The apparent surface free energy of rare earth oxides is governed by hydrocarbon, Adsorpt. Isc. 25 (2021), 103691, https://doi.org/10.1016/j.isci.2021.103691.
[28] J. Tam, B. Feng, Y. Ikuhara, H. Ohta, U. Erb, Crystallographic orientation-surface energy-wetting property relationships of rare earth oxides, J. Mater. Chem. A 6 (2018) 18384–18388, https://doi.org/10.1039/C8TA04938F.
[29] K. Nakayama, T. Hiraga, C. Zhu, E. Tsuji, Y. Aoki, H. Habazaki, Facile preparation of self-healing superhydrophobic CeO2 surface by electrochemical processes, Appl. Surf. Sci. 423 (2017) 968–976, https://doi.org/10.1016/j.apsusc.2017.07.012.
[30] J. Bae, I.A. Samek, P.C. Stair, R.Q. Snurr, Investigation of the hydrophobic nature of metal oxide surfaces created by atomic layer deposition, Langmuir 35 (2019) 5762–5769, https://doi.org/10.1021/acs.langmuir.9b00577.
[31] A. Kozbial, Z. Li, J. Sun, X. Gong, F. Zhou, Y. Wang, H. Xu, H. Liu, L. Li, Understanding the intrinsic water wettability of graphite, Carbon 74 (2014) 218–225, https://doi.org/10.1016/j.carbon.2014.03.025.
[32] J. Yuan, X. Liu, O. Akbulut, J. Hu, S.L. Suib, J. Kong, F. Stellacci, Superwetting nanowire membranes for selective absorption, Nat. Nanotechnol. 3 (2008) 332–336, https://doi.org/10.1038/nnano.2008.136.
[33] S. Vudayagiri, M.D. Junker, A.L. Skov, Factors affecting the surface and release properties of thin polydimethylsiloxane films, Polym. J. 45 (2013) 871–878, https://doi.org/10.1038/pj.2012.227.
[34] M.V. Dover, W.A. Hensley, Properties of 1-Octadecene, n-Octadecane, and Di-m-tolylethane, Ind. Eng. Chem. 27 (1935) 337–339, https://doi.org/10.1021/ie50303a023.
[35] D.G. Branco, C.A. Santiago, F.J. Oliveira, L. Cabrita, D.V. Evtuguin, Surface properties of cork in relation to reactive washing, Colloids Surf. A Physicochem. Eng. Asp. 624 (2021), 126762, https://doi.org/10.1016/j.colsurfa.2021.126762.
[36] D. Zhu, W. Liu, R. Zhao, Z. Shi, X. Tan, Z. Zhang, Y. Li, L. Ji, X. Zhang, Microscopic insights into hydrophobicity of cerium oxide: effects of crystal orientation and lattice constant, J. Mater. Sci. Technol. 109 (2022) 20–29, https://doi.org/10.1016/j.jmst.2021.08.064.
[37] D. Mamedov, S.Z. Karazhanov, Doping-induced modulation of electronic, optical and wetting properties of CeO_2, J. Phys. Chem. Solids 168 (2022), 110820, https://doi.org/10.1016/J.JPCS.2022.110820.
[38] S. Van Steenberge, W.P. Leroy, D. Depla, Influence of oxygen flow and film thickness on the texture and microstructure of sputtered ceria thin films, Thin Solid Films 553 (2014) 2–6, https://doi.org/10.1016/j.tsf.2013.11.049.
[39] T. An, X. Deng, S. Liu, S. Wang, J. Ju, C. Dou, Growth and roughness dependent wetting properties of CeO_2 films prepared by glancing angle deposition, Ceram. Int. 44 (2018) 9742–9745, https://doi.org/10.1016/j.ceramint.2018.02.206.
[40] D. Zhu, C. Hu, R. Zhao, X. Tan, Y. Li, V. Mandić, Z. Shi, X. Zhang, Fabrication of cerium oxide films with thickness and hydrophobicity gradients, Surf. Coat. Technol. 430 (2022), https://doi.org/10.1016/j.surfcoat.2021.127985.
[41] Z. Shi, P. Shum, Z. Zhou, L.K.Y. Li, Effect of bias voltage on the properties of CeO_{2-x} coatings prepared by magnetron sputtering, Surf. Coat. Technol. 326 (2017) 411–416, https://doi.org/10.1016/j.surfcoat.2016.11.104.
[42] Z. Shi, P. Shum, Z. Zhou, L.K.Y. Li, Effect of oxygen flow ratio on the wetting behavior, microstructure and mechanical properties of CeO_{2-x} coatings prepared by magnetron sputtering, Surf. Coat. Technol. 320 (2017) 333–338, https://doi.org/10.1016/j.surfcoat.2016.12.055.
[43] M. Jorge, S. Cooil, M.T. Edmonds, L. Thomsen, M. Nematollahi, F. Mazzola, J. W. Wells, Accelerated ageing of molybdenum oxide, Mater. Res. Express 4 (2017), 115502, https://doi.org/10.1088/2053-1591/aa9287.
[44] S. Khan, G. Azimi, B. Yildiz, K.K. Varanasi, Role of surface oxygen-to-metal ratio on the wettability of rare-earth oxides, Appl. Phys. Lett. 106 (2015) 2–7, https://doi.org/10.1063/1.4907756.
[45] L. Martínez, E. Román, J.L. de Segovia, S. Poupard, J. Creus, F. Pedraza, Surface study of cerium oxide based coatings obtained by cathodic electrodeposition on zinc, Appl. Surf. Sci. 257 (2011) 6202–6207, https://doi.org/10.1016/j.apsusc.2011.02.033.
[46] E.J. Preisler, O.J. Marsh, R.A. Beach, T.C. McGill, Stability of cerium oxide on silicon studied by x-ray photoelectron spectroscopy, J. Vac. Sci. Technol. B Microelectron. Nanom. Struct. Process. Meas. Phenom. 19 (2001) 1611–1618, https://doi.org/10.1116/1.1387464.
[47] K.I. Maslakov, Y.A. Teterin, A.J. Popel, A.Y. Teterin, K.E. Ivanov, S.N. Kalmykov, V. G. Petrov, P.K. Petrov, I. Farnan, XPS study of ion irradiated and unirradiated CeO_2 bulk and thin film samples, Appl. Surf. Sci. 448 (2018) 154–162, https://doi.org/10.1016/j.apsusc.2018.04.077.
[48] T.L. Barr, S. Seal, Nature of the use of adventitious carbon as a binding energy standard, J. Vac. Sci. Technol. A 13 (1995) 1239–1246, https://doi.org/10.1116/1.579868.
[49] A. Fujimori, Mixed-valent ground state of CeO_2, Phys. Rev. B 28 (1983) 2281–2283, https://doi.org/10.1103/PhysRevB.28.2281.
[50] A. Marmur, The lotus effect: superhydrophobicity and metastability, Langmuir 20 (2004) 3517–3519, https://doi.org/10.1021/la036369u.
[51] P.K. Basu, D. Sarangi, K.D. Shetty, M.B. Boreland, Liquid silicate additive for alkaline texturing of mono-Si wafers to improve process bath lifetime and reduce IPA consumption, Sol. Energy Mater. Sol. Cells 113 (2013) 37–43, https://doi.org/10.1016/j.solmat.2013.01.037.
[52] J. Thorstensen, J. Gljessing, E.S. Marstein, S.E. Foss, Light-trapping properties of a diffractive honeycomb structure in silicon, IEEE J. Photovolt. 3 (2013) 709–715, https://doi.org/10.1109/JPHOTOV.2013.2240563.